ARTICLE   OPEN

Bound state in a giant atom-modulated resonators system

Han Xiao [ID][1,7], Luojia Wang[1,7], Zheng-Hong Li [ID][2,3 ✉], Xianfeng Chen [ID][1,4,5,6] and Luqi Yuan [ID][1 ✉]

It is of fundamental interest in controlling the light–matter interaction for a long time in the field of quantum information processing. Here, we explore a model by coupling a giant atom with the dynamically-modulated coupled-resonator waveguide and find the bound state, where the light shows the localization effect and the atomic decay into resonator modes is inhibited, excited by a propagating photon. An analytical treatment based on the separation of the propagating states and localized states of light has been proposed and provides inspiring explanation of our finding, i.e., there supports a quantum channel where the propagating photon can be converted to the localized state through the quantum interference from light–atom interactions in three resonators at different frequency detunings. Our work therefore shows the potential for actively localizing the photon in a modulated coupled-resonator waveguide system interacting with the giant atom, and also points out a way to study the light–atom interaction in a synthetic frequency dimension that holds the similar Hamiltonian.

INTRODUCTION

It is of great importance in achieving flexible manipulations of photons in atom-waveguide systems and exploring fundamental physics associated with strong light–atom interactions and atom-mediated photon–photon interactions, which also shows potential applications towards quantum communications and quantum networks[1–13]. Similar with but different from the continuum waveguide, the coupled-resonator waveguide provides an alternative structure for manipulating the spatial and spectral properties of photons, where photon transport can be controlled by designing combinations of resonators with the nonlinearity of the resonator[14–19] or by actively connecting resonators with dynamic modulations[20–22]. In both cases, atoms (or quantum emitters) can be added into the coupled-resonator waveguide and hence further possible controllability of photons has been discussed[23–28]. Although theoretical models may be originally studied in photonic structures, such coupled-resonator waveguide has also been discussed in the on-chip platform of superconducting transmission line resonators[29–31], where microwave photons transport and can be interacting with the artificial superconducting qubit[26,32–34].

Recently, the atom-waveguide system has been generalized to studies of interactions between the photon in the waveguide and a giant atom, where an artificial atom (quantum emitter) is fabricated to couple multiple locations on the waveguide[35]. Due to the fact that multi-path quantum interferences are included in interactions between waveguide photons and giant atoms, a variety of interesting quantum optical phenomena have been explored, including bound states or dressed states[28,36–39], decoherence-free interaction[40–43], electromagnetically-induced transparency[44–47], and many others[48–56]. Relevant experiments have also been demonstrated that microwave photons or propagating phonons have been successfully coupled to an artificial gaint atom[41,45,57]. Hence, explorations of different opportunities in seeking exotic manipulations of photons via quantum interferences from the photon–giant-atom interaction in the coupled-resonator waveguide trigger further theoretical interests.

In this work, we study a theoretical model of an artificial two-level giant atom coupled with dynamically-modulated coupled-resonator waveguide (see Fig. 1), where each resonator (labeled by m) supports a resonant mode at the frequency $\omega_m = \omega_0 + m\Omega$ with ω_0 being the transition frequency of the atom. The giant atom couples to the middle three resonators (0-th and ±1-st) through three separate paths. We find that, for the choice of modulation parameters, the wavepacket of the photon that transports inside the waveguide exhibits the localization effect, together with the time of the photon–atom interaction lasting longer than the decay rate between the atom and the resonator, i.e., namely bound state. The key feature here is the excitation of a bound state corresponding to photon modes with group velocities close to zero by the traveling photon, which is counter-intuitive. We provide the analytical analysis based on the separation of propagating states and localized states of light, and find the quantum transition channel from propagating states to localized states. Moreover, our studied Hamiltonian also describes an artificial lattice in the synthetic frequency dimension[58–61], which could trigger further research interest in the photon–atom interaction with synthetic dimensions. Therefore, this work shows the photon manipulation through quantum interferences in a system composed by the giant atom and the dynamically-modulated coupled-resonator waveguide, which shall find potential applications in the quantum information processing[62,63].

RESULTS

Model

As schematically shown in Fig. 1, we consider a one-dimensional photonic resonator lattice, with each resonator supporting a single resonance at ω_m. The dynamic modulation can be applied in-between two adjacent resonators by modulating two resonances
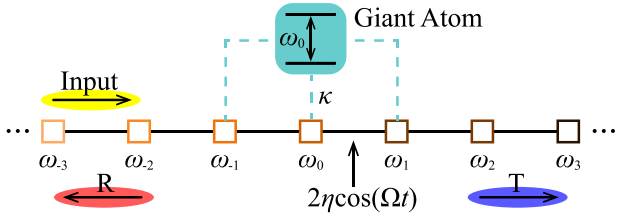
Fig. 1 Schematics for a 1D dynamically-modulated coupled-resonator waveguide coupling to a two-level giant atom. The excited source is injected into the waveguide (yellow). After it interacting with the giant atom, the field is transmitted (blue) or reflected (red).

in the auxiliary resonator with a sinusoid external source $2\eta\cos\Omega t$ where $\Omega \ll \omega_0$ is the frequency and η is the modulation amplitude[20,64]. A two-level giant atom is designed to couple with the 0-th and ±1-st resonators with the coupling strength κ. By assuming $\hbar = 1$, the corresponding Hamiltonian is

$$H = \omega_0 \frac{\sigma_z}{2} + \sum_m \omega_m a_m^\dagger a_m + \sum_m 2\eta\cos(\Omega t)(a_m^\dagger a_{m+1} + a_{m+1}^\dagger a_m)$$
$$+ \sum_{m'=-1,0,1} \kappa(a_{m'}^\dagger \sigma_- + a_{m'}\sigma_+). \tag{1}$$

Here, $\sigma_z = [\sigma_+, \sigma_-]$. $\sigma_+ = |e\rangle\langle g|$ ($\sigma_- = |g\rangle\langle e|$) is the ladder operator that transits the atom from ground state $|g\rangle$ to excited state $|e\rangle$ (and vice versa), and $a_m^\dagger$ (a_m) is the creation (annihilation) operator for the photon in the m-th resonator. One can rewrite the Hamiltonian in the interaction picture under the rotating-wave approximation (RWA)[65]

$$V(t) = \sum_m \eta\left(a_m^\dagger a_{m+1} + a_{m+1}^\dagger a_m\right) + \sum_{m'=-1,0,1} \kappa\left(a_{m'}^\dagger \sigma_- e^{im'\Omega t} + a_{m'}\sigma_+ e^{-im'\Omega t}\right). \tag{2}$$

To simulate the dynamics of photon transport, we write the single-excitation wave function

$$|\psi(t)\rangle = \sum_m v_m(t) a_m^\dagger |0, g\rangle + \xi(t)|0, e\rangle, \tag{3}$$

where v_m is the probability amplitude for creating the photon from the vacuum state $|0\rangle$ in the m-th resonator while the atom remains at the ground state $|g\rangle$, and ξ is the probability amplitude for the atom being excited (to $|e\rangle$) by the propagating photon. By using the Schrödinger's equation, we obtain

$$\dot{v}_m = -i\eta(v_{m+1} + v_{m-1}) - i\kappa \sum_{m'=-1,0,1} \xi e^{im'\Omega t}\delta_{m,m'}, \tag{4}$$

$$\dot{\xi} = -i\kappa \sum_{m'=-1,0,1} v_{m'} e^{-im'\Omega t}. \tag{5}$$

In simulations, we consider a coupled-resonator waveguide composed by 401 resonators ($m = -200, \cdots, 200$). A Gaussian-shape pulse $S = e^{-(t-t_0)^2/\tau^2}$ is used to excite the leftmost resonator, where $\tau = 5\sqrt{2}\eta^{-1}$ and $t_0 = 25\eta^{-1}$. We first consider the case that $\kappa = 0.5\eta$ and $\Omega = 3\eta$. In Fig. 2a, we plot the distribution of $|v_m|^2$ on different resonators and $|\xi|^2$ versus the time t. One sees that the photon is injected into the system from the left and then propagates towards the right. Once it interacts with the atom, a portion of the wavepacket of the photon is reflected while the atom is excited, which shows consistence with the propagating photon interacting with a resonant atom in a waveguide[66,67]. The striking feature of the system is found when we choose $\Omega = 2.05\eta$ while keeping other parameters unchanged, with simulation results plotted in Fig. 2b. One sees that, once the light

interacts with the atom, the wavepacket of the photon is stored for a relative long time in the vicinity of middle resonators ($\sim150\eta^{-1} \gg \kappa^{-1}$) and the excitation of the atom also gives a relative long decay tail. Such the phenomenon denotes a bound state of photon and atom where the light shows the localization effect near middle resonators and atom exhibits the inhibited decay. Besides the bound state, together with the transmission of a portion of wavepacket at the original group velocity, other small portions of wavepacket are transmitted and reflected at a smaller group velocity. By further studying cases for Ω nearby 2.05η, we find that the existence of the bound state is critically dependent on the choice of Ω (see Supplementary Note 1 for details), with detailed physical mechanism will be analyzed analytically in the following.

Analytical analysis
In order to understand the bound state in our proposed model, we next analyze the Hamiltonian (2) analytically in details. The first term in Eq. (2) gives couplings between resonators driven by an external source, while the second term describes atom–resonator interactions, where $\pm\Omega$ represents the detuning between the ±1-st resonator and the atom. Since the atom only couples with the middle three resonators, and we consider a finite number of resonators ($-M \le m < M$ with M being a positive integer), the influence of the photon state in resonators at two boundaries is negligible for $M \gg 1$. We hence can take the state $|k\rangle = \sum_{m=-M}^{M-1} a_m^\dagger |0\rangle e^{imk\pi/M}/\sqrt{2M}$ ($k = -M, \cdots, M-1$ as an integer) in the momentum space which is the eigenstate of $\sum_{m=-M}^{M-1} \eta(a_m^\dagger a_{m+1} + \text{h.c.})$ and is regarded as the Bloch wave in the lattice with the frequency $\omega_k = 2\eta\cos(k\pi/M)$. Note here we set the spatial distance between two resonators as 1 for the simplicity. The corresponding group velocity of the wavepacket is $v_k = -2\eta\sin(k\pi/M)$. Obviously, when $\omega_k = \pm2\eta$, the wavepacket has the group velocity $v_k = 0$ and therefore does not move in the lattice. We will refer to them as localized modes in the following discussions.

Along with the atomic states $|e\rangle$ and $|g\rangle$, now we can rewrite V in the k-space, which leads to $\tilde{V} = \tilde{V}_0 + \tilde{V}_1$. Here

$$\tilde{V}_0 = \sum_{k=-M}^{M-1} \omega_k |k\rangle\langle k|, \tag{6}$$

$$\tilde{V}_1 = \sum_{k=-M}^{M-1} \sum_{m'=-1}^{1} \frac{\kappa}{\sqrt{2M}}\left(e^{-i\frac{m'k\pi}{M}} e^{im'\Omega t}|k, g\rangle\langle 0, e| + \text{h.c.}\right). \tag{7}$$

In the interaction-picture Hamiltonian under the k representation, i.e.,

$$e^{i\tilde{V}_0 t}\tilde{V}_1 e^{-i\tilde{V}_0 t} = \sum_{k=-M}^{M-1} \sum_{m'=-1}^{1} \frac{\kappa}{\sqrt{2M}}\left(e^{-i\frac{m'k\pi}{M}} e^{i(m'\Omega + \omega_k)t}|k, g\rangle\langle 0, e| + \text{h.c.}\right), \tag{8}$$

one clearly sees that each state $|k\rangle$ interacts with the atom through the middle three resonators with $m' = 0, \pm1$, while $m'\Omega + \omega_k$ represents the detuning between the atom and the Bloch-wave state for the m'-th resonator. Following this argument, we can assume that each state $|k\rangle$ is only coupled with the resonator with the smallest detuning. Hence, we obtain the Hamiltonian as

$$\tilde{V} \approx \sum_{k=-M}^{M-1} \omega_k |k\rangle\langle k| + \frac{\kappa}{\sqrt{2M}} \sum_{m'=-1}^{1}\left(\sum_{k\in K_m} e^{-i\frac{m'k\pi}{M}} e^{im'\Omega t}|k, g\rangle\langle 0, e| + \text{h.c.}\right), \tag{9}$$

where we divide k into three regions. In region K_0, the photon state of the Bloch wave has $\omega_k \in (-\sqrt{2}\eta, \sqrt{2}\eta)$, and is only coupled with the 0-th resonator. Similarly, in region $K_{\pm1}$, $\omega_k \in (\mp\sqrt{2}\eta, \mp2\eta]$, and the photon state is coupled with the ±1-st resonator. We emphasize that, according to the resonance condition ($m'\Omega + \omega_k = 0$), the photon state that make most contributions have frequencies $\omega_k = 0, \pm2\eta$. Therefore, except for
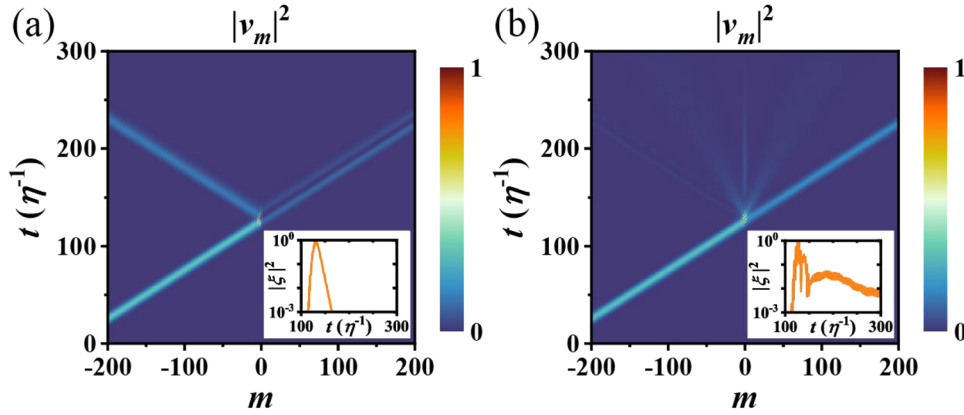
Fig. 2 The evolution of photonic states. Normalized probability distributions of photon in different resonators versus the time, when (**a**) $\Omega = 3\eta$ and (**b**) $\Omega = 2.05\eta$, respectively. The insets show the corresponding normalized atomic excitation probability in the logarithm scale.

the states near these three frequencies, other states in the k-space are negligible in our analytical analysis, and the choice of the limit of the above-mentioned regions is for the convenience purpose.

The wave function of the photon state in the k-space has the form

$$|\psi(t)\rangle_k = \sum_{k=-M}^{M-1} C_k(t)|k,g\rangle + \chi(t)|0,e\rangle, \quad (10)$$

and together with Eq. (9), we can get the corresponding dynamic evolution equations. However, we notice that, there are 4 corresponding states $|k\rangle$ at each $|\omega_k|$. For the sake of simplicity, we hence define linear combinations of states for the same $|\omega_k|$:

$$J_{k,s\pm}(t) = \frac{1}{2}\left\{\left[C_k(t)e^{-\frac{ik\pi}{M}} + C_{-k}(t)e^{\frac{ik\pi}{M}}\right]e^{i\Omega t}\right.$$
$$\left.\pm \left[C_{M-k}(t)e^{i(\pi-\frac{k\pi}{M})} + C_{-(M-k)}(t)e^{-i(\pi-\frac{k\pi}{M})}\right]e^{-i\Omega t}\right\}, \quad (11)$$

$$J_{k,0\pm}(t) = \frac{1}{2}\left\{\left[C_{M/2-k}(t) + C_{-(M/2-k)}(t)\right] \pm \left[C_{M/2+k}(t) + C_{-(M/2+k)}(t)\right]\right\}, \quad (12)$$

with $k \in [0, M/4)$, and obtain

$$i\frac{\partial}{\partial t}J_{k,s+}(t) = \frac{2\kappa}{\sqrt{2M}}\chi(t) - (\Omega - \omega_k)J_{k,s-}(t), \quad (13)$$

$$i\frac{\partial}{\partial t}J_{k,s-}(t) = -(\Omega - \omega_k)J_{k,s+}(t), \quad (14)$$

$$i\frac{\partial}{\partial t}\chi(t) = \frac{\kappa}{\sqrt{2M}}\left[J_{0,s+}(t) + 2\sum_{k=1}^{M/4-1}J_{k,s+}(t)\right]$$
$$+ \frac{\kappa}{\sqrt{2M}}\left[J_{0,0+}(t) + 2\sum_{k=1}^{M/4-1}J_{k,0+}(t)\right], \quad (15)$$

$$i\frac{\partial}{\partial t}J_{k,0+}(t) = \frac{2\kappa}{\sqrt{2M}}\chi(t) - v_k J_{k,0-}(t), \quad (16)$$

$$i\frac{\partial}{\partial t}J_{k,0-}(t) = -v_k J_{k,0+}(t). \quad (17)$$

Here $J_{k,s\pm}$ ($k \in [0, M/4)$) denotes the modes of the photon state whose group velocity is in the range of $(\pm\sqrt{2}\eta, 0]$ (where $J_{0,s\pm}$ corresponds to modes with $v_k = 0$, i.e., localized states), and $J_{k,0\pm}$ denotes those modes whose group velocities $v_k \in (\pm\sqrt{2}\eta, \pm 2\eta]$ (where $J_{0,0\pm}$ corresponds to modes with $v_k = \pm 2\eta$, i.e., propagating states). Eqs. (13)–(17) indicate that $J_{k,s\pm}$ and $J_{k,0\pm}$ form two sets of

subsystems, connected by the atom [see Eq. (15)]. We then focus on the subsystem described by Eqs. (13)–(15), where localized modes are included. In order to erase the impact of the other subsystem, we discard the second term on the right-hand side of Eq. (15). Then, by setting that $J_{k,s\pm}(t) = j_{k,s\pm}e^{-i\lambda_s t}$ and $\chi(t) = x_s e^{-i\lambda_s t}$, we find the special solution with $\lambda_s = 0$, which gives

$$x_s = \frac{\sqrt{2M}}{2\kappa}(\Omega - \omega_k)j_{k,s-}, \quad (18)$$

$$j_{k,s+} = 0. \quad (19)$$

Equations (18), (19) are solvable with the normalization condition involved. Equation (18) suggests that when $\Omega > 2\eta$, $|j_{k,s-}|$ decreases as k increases, which implies that the mode distribution of the photon state is concentrated near $\omega_k = \pm 2\eta$. Notice that $|j_{k,s-}|$ is proportional to $|x_s|$. Once the atom is excited, it is possible to observe the localized state with $v_k = 0$. This is a bound state in which the photon is stored and the atom keeps excited with the inhibited decay. However, we need to point out that when Ω becomes large, the proportion of the atomic excited state in the bound state is also increasing. Due to normalization condition, the probability that the system is in the localized state in the vicinity of $k = 0$ is suppressed. On the other hand, when $\Omega < 2\eta$, $|j_{k,s-}|$ increases as k increases, and hence the maximum value of $|j_{k,s-}|$ is at $k \neq 0$ ($v_k \neq 0$). In such case, the localized state is nearly impossible to be generated. Therefore, we only have a very narrow window of Ω to obtain a significant localized photon state, which is consistent with our previous numerical results.

The above discussion shows that through the interaction with the ± 1-st resonators and the atom, the photon may move slowly or even stay localized in the waveguide. The next question is how to excite such localized state, since the initial wavepacket of the photon is prepared centered at $\omega_k = 0$ with spectral width $\sim 1/\tau$ nearly does not contain any component of $\omega_k = \pm 2\eta$ ($v_k = 0$). From Eq. (15), one finds that the coupling strengths of the two subsystems and the atom are similar, which means that the effects of the two subsystems on the atom are comparable. Consequently, we have the following physical picture: An initial state of the photon is prepared in one subsystem (corresponding to $J_{k,0\pm}$) where the center frequency of the initial wavepacket is $\omega_k = 0$ and $v_k \sim 2\eta$ for example. Such wavepacket of the photon propagates inside the waveguide and causes the excitation of the atom, which in turn leads to the excitation of another subsystem (corresponding to $J_{k,s\pm}$), i.e., creating the bound state with the localized photon state and an excited atom lasting for a long time. This picture is consistent with our simulation result in Fig. 2b.
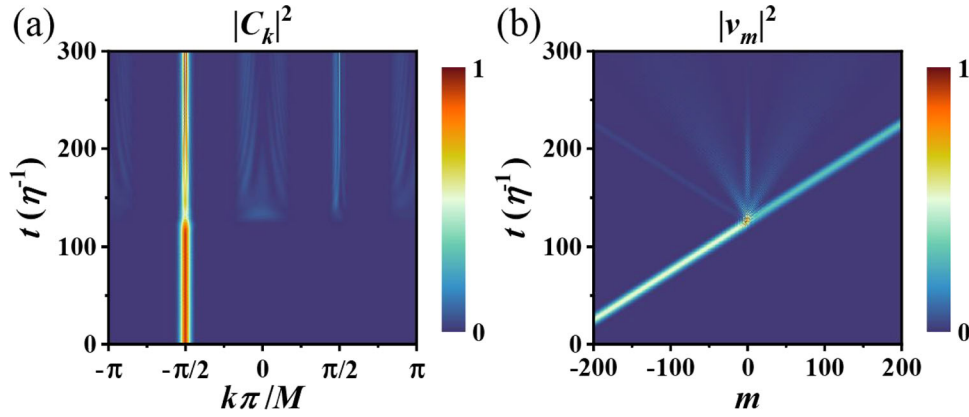
Fig. 3 The generation of photonic bound states in the *k*-space. a Normalized wave function of the photon in the *k*-space. **b** The normalized probability distribution of photon in different resonators versus the time. In both figures, simulations are performed in the *k*-space with $\Omega = 2.05\eta$.

Finally, we perform simulations in the *k*-space with the separation approximation that we analytically discussed above to verify our analytical analysis. By combining Eq. (9) and the Schrödinger's equation, we simulate the evolution of the states in the *k*-space over time with $\Omega = 2.05\eta$ and plot the result in Fig. 3a. The initial state of the system is assumed to be a Gaussian wavepacket in real space, with its center position at $m_0 = -250$ and propagating toward the right at a group velocity 2η, i.e., $|\psi_I\rangle = \sum_{m=-M}^{M} e^{-(m-m_0)^2/2\delta_m^2} e^{-i\pi(m-m_0)/2} |m\rangle$, with $\delta_m = 10$. (This choice of the initial wavepacket is consistent with the boundary-excitation source in simulations for Fig. 2) Therefore, the Fourier transformation of the initial state (with taking $M = 500$) here gives the initial wave function in Eq. (10) for simulations, with the central momentum being $k\pi/M = -\pi/2$. Figure 3a indicates that the mode separation approximation we used in the above discussion is feasible, because one can see that the energy distribution of the photon's wavepacket is centered near $k\pi/M = -\pi, -\pi/2, 0, \pi/2$ with clear separations. Next, we follow the mode separation approximation and use Eqs. (13)–(17) with the same parameters for Fig. 3a and numerically calculate the photon distribution in the *k*-space. After we Fourier-transform the simulation results back into the real space, we plot the resulting probability distribution of photon in Fig. 3b. One can see that evolutions of the photon in both Figs. 3b, 2b match quite well, indicating our analytical analysis is valid in understanding such light localization phenomenon.

DISCUSSION

There are several notes we want to provide further discussions. Different from previous works studying bound states in atom-waveguide systems using either giant atoms[36] or small atoms[68,69], the energy of bound states is explicitly out of the regime for the propagating band of the waveguide. Hence, it is fundamentally difficult to excite such photonic bound states through the propagating waveguide photon. On the contrary, in our model, we find that the coupling between the giant atom and the 0-th resonator provides the excitation of giant atom and the couplings between the ±1-st resonators converts the atomic excited state to a hybrid bound state, which shows the possibility for exciting a bound state by the propagating photon without using external drive fields (see Supplementary Note 2 for details). This unique feature therefore provides potential important applications in quantum storage. Moreover, in simulations, we use an initial Gaussian-shape excitation to provide the input pulse of the incoming propagating photon, where a narrow spectrum of the

input wavepacket is used to excite the giant atom. For seeing clear effects of the propagating photon and the light localization, we use the waveguide with hundreds of resonators. In reality, a shorter waveguide with tens of resonators is also feasible, as long as it can carry the entire single-photon pulse before the photon interacting the giant atom. In this case, one can inject the waveguide at the end of resonator from outer connecting waveguide where the effect of boundary reflections should be negligible. As an example, in Supplementary Note 3, we study the case of exciting the waveguide consisting 21 resonators with the same Gaussian-shape input photon source, and see the bound state still existing, which is experimentally feasible[69]. The energy distribution of such bound state could be further enhanced by increasing the full width at half maximum of the Gaussian-shape pulse, which corresponds to a narrower width in the spectrum and larger portion of the wavepacket can then interact with the giant atom to excite the bound state. In Supplementary Note 4, we showcase the result with $\tau = 10\sqrt{2}\eta^{-1}$ where a significant increase in the energy distribution of the photonic localized state together with the extension of the inhibited atomic decay time exists.

Before we conclude our paper, we point out that our studied model naturally supports a synthetic lattice along the frequency axis of light, which is constructed in a modulated ring resonator and is similarly described by the Hamiltonian $\sum_m \omega_m a_m^\dagger a_m + \sum_m 2\eta \cos(\Omega t)(a_m^\dagger a_{m+1} + a_{m+1}^\dagger a_m)$ (the same as with the waveguide part in Eq. (1) with ω_m being resonant frequencies and Ω being the frequency of the modulator[61]. Once a two-level atom at the transition frequency ω_0 is added to couple with the ring, an effective giant atom coupled with the synthetic lattice with the linear-gradient detuning $(\omega_m - \omega_0)$ at each connection is built, as shown in Fig. 4. We find that the affects from far-from-resonance couplings weakly affect the system, and our findings in this work shall also map to the dynamics in the synthetic dimension (see Supplementary Note 5 for details). However, detailed consequences in the output of the single-photon spectrum desires further studies with the input-output formalism carefully included, which is beyond the scope of this paper. Yet, our work is still useful in the future understanding of the photon-transport problem with the recent-developed synthetic dimensions[70–72] coupled to a atom, which opens an avenue to study quantum optics in a synthetic waveguide coupled with an effective giant atom with coupling positions reaching the order of 10^3 [73].

In summary, we study the photon propagation problem inside a coupled-resonator waveguide under the dynamic modulation with the middle three resonators coupled with the giant atom,
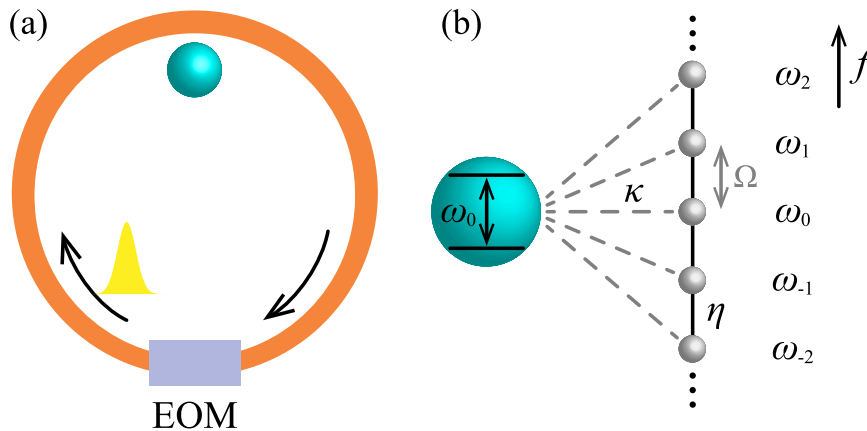
Fig. 4 Schematics for an effective giant atom coupling with a synthetic frequency waveguide. a Schematic for a dynamically-modulated ring resonator coupling to a two-level giant atom. EOM denotes to the electro-optic modulator. **b** The two-level atom coupled with the lattice in the synthetic frequency dimension supporting a giant atom with detuned connections.

where the dynamic modulation frequency precisely equals to the frequency difference between two nearby resonators. We find that, through multi-resonator couplings, one can excite the Bloch-wave state in the system by a propagating input photon, so the light field can be localized for a long time and the excitation of the atom exhibits the inhibited decay. An analytical approach is built to understand the intrinsic quantum interference dynamics. Our model is valid for a variety of potential experimental platforms, including photonic-crystal waveguide[20,74], coupled cavities in free space[75,76], superconducting transmission line resonators[77–80]. Moreover, such a model can also be useful in understanding a synthetic lattice along the frequency axis of light coupling to a two-level atom that has the similar Hamiltonian. The bound states with near zero group velocity for photons localize the energy of information and has extensive applications in quantum storages[81,82]. Our work therefore shows a theoretical perspective for studying photon–atom interactions in waveguide systems and seeks additional external control of the propagating photon, which can find applications in quantum manipulations of a single photon.

Note.—When we prepare our paper, we notice an independent preprint, which is related but different from our work[83].

DATA AVAILABILITY

The data files used to prepare the figures shown in the paper are available from corresponding authors upon request.

CODE AVAILABILITY

The codes that support the findings of this study are available from corresponding authors upon request.

REFERENCES

1. Goban, A. et al. Superradiance for atoms trapped along a photonic crystal waveguide. *Phys. Rev. Lett.* **115**, 063601 (2015).
2. Yuan, L., Xu, S. & Fan, S. Achieving nonreciprocal unidirectional single-photon quantum transport using the photonic Aharonov-Bohm effect. *Opt. Lett.* **40**, 5140–5143 (2015).
3. Pichler, H. & Zoller, P. Photonic circuits with time delays and quantum feedback. *Phys. Rev. Lett.* **116**, 093601 (2016).
4. Forn-Díaz, P. et al. Ultrastrong coupling of a single artificial atom to an electro-magnetic continuum in the nonperturbative regime. *Nat. Phys.* **13**, 39–43 (2017).
5. Cheng, M.-T., Ma, X., Fan, J.-W., Xu, J. & Zhu, C. Controllable single-photon non-reciprocal propagation between two waveguides chirally coupled to a quantum emitter. *Opt. Lett.* **42**, 2914–2917 (2017).
6. Kumlin, J., Hofferberth, S. & Büchler, H. P. Emergent universal dynamics for an atomic cloud coupled to an optical waveguide. *Phys. Rev. Lett.* **121**, 013601 (2018).
7. Mahmoodian, S. et al. Strongly correlated photon transport in waveguide quantum electrodynamics with weakly coupled emitters. *Phys. Rev. Lett.* **121**, 143601 (2018).
8. Corzo, N. V. et al. Waveguide-coupled single collective excitation of atomic arrays. *Nature* **566**, 359–362 (2019).
9. Mirhosseini, M. et al. Cavity quantum electrodynamics with atom-like mirrors. *Nature* **569**, 692–697 (2019).
10. Xiao, H., Wang, L., Yuan, L. & Chen, X. Frequency manipulations in single-photon quantum transport under ultrastrong driving. *ACS Photonics* **7**, 2010–2017 (2020).
11. Kim, E. et al. Quantum electrodynamics in a topological waveguide. *Phys. Rev. X* **11**, 011015 (2021).
12. Poshakinskiy, A. V. et al. Quantum Hall phases emerging from atom-photon interactions. *NPJ Quantum Inf.* **7**, 34 (2021).
13. Nefedkin, N., Cotrufo, M., Krasnok, A. & Alù, A. Dark-state induced quantum nonreciprocity. *Adv. Quantum Technol.* **5**, 2100112 (2022).
14. Marin-Palomo, P. et al. Microresonator-based solitons for massively parallel coherent optical communications. *Nature* **546**, 274–279 (2017).
15. Stern, B., Ji, X., Okawachi, Y., Gaeta, A. L. & Lipson, M. Battery-operated integrated frequency comb generator. *Nature* **562**, 401–405 (2018).
16. Zhang, M. et al. Broadband electro-optic frequency comb generation in a lithium niobate microring resonator. *Nature* **568**, 373–377 (2019).
17. Lu, J. et al. Periodically poled thin-film lithium niobate microring resonators with a second-harmonic generation efficiency of 250,000%/W. *Optica* **6**, 1455–1460 (2019).
18. Szabados, J. et al. Frequency comb generation via cascaded second-order non-linearities in microresonators. *Phys. Rev. Lett.* **124**, 203902 (2020).
19. Yu, S.-P. et al. Spontaneous pulse formation in edgeless photonic crystal resonators. *Nat. Photonics* **15**, 461–467 (2021).
20. Fang, K., Yu, Z. & Fan, S. Realizing effective magnetic field for photons by controlling the phase of dynamic modulation. *Nat. Photon.* **6**, 782–787 (2012).
21. Fang, K. & Fan, S. Controlling the flow of light using the inhomogeneous effective gauge field that emerges from dynamic modulation. *Phys. Rev. Lett.* **111**, 203901 (2013).
22. Williamson, I. A. D. et al. Integrated nonreciprocal photonic devices with dynamic modulation. *Proc. IEEE* **108**, 1759–1784 (2020).
23. Hoffman, A. J. et al. Dispersive photon blockade in a superconducting circuit. *Phys. Rev. Lett.* **107**, 053602 (2011).
24. Zhou, L., Yang, L.-P., Li, Y. & Sun, C. P. Quantum routing of single photons with a cyclic three-level system. *Phys. Rev. Lett.* **111**, 103604 (2013).
25. Lu, J., Zhou, L., Kuang, L.-M. & Nori, F. Single-photon router: coherent control of multichannel scattering for single photons with quantum interferences. *Phys. Rev. A* **89**, 013805 (2014).

26. Fitzpatrick, M., Sundaresan, N. M., Li, A., Koch, J. & Houck, A. A. Observation of a dissipative phase transition in a one-dimensional circuit QED lattice. *Phys. Rev. X* **7**, 011016 (2017).

27. Wang, L., Yuan, L., Chen, X. & Fan, S. Single-photon transport in a topological waveguide from a dynamically modulated photonic system. *Phys. Rev. Appl.* **14**, 014063 (2020).

28. Wang, X., Liu, T., Kockum, A. F., Li, H.-R. & Nori, F. Tunable chiral bound states with giant atoms. *Phys. Rev. Lett.* **126**, 043602 (2021).

29. Devoret, M. H., Girvin, S. & Schoelkopf, R. Circuit-QED: how strong can the coupling between a Josephson junction atom and a transmission line resonator be? *Ann. Phys.* **16**, 767–779 (2007).

30. Gu, X., Kockum, A. F., Miranowicz, A., Liu, Y.-x & Nori, F. Microwave photonics with superconducting quantum circuits. *Phys. Rep.* **718–719**, 1–102 (2017).

31. Blais, A., Grimsmo, A. L., Grivin, S. M. & Wallraff, A. Circuit quantum electro-dynamics. *Rev. Mod. Phys.* **93**, 025005 (2021).

32. Hoi, I.-C. et al. Demonstration of a single-photon router in the microwave regime. *Phys. Rev. Lett.* **107**, 073601 (2011).

33. Stockklauser, A. et al. Strong coupling cavity QED with gate-defined double quantum dots enabled by a high impedance resonator. *Phys. Rev. X* **7**, 011030 (2017).

34. Yan, Z. et al. Strongly correlated quantum walks with a 12-qubit superconducting processor. *Science* **364**, 753–756 (2019).

35. Kockum, A. F., Delsing, P. & Johansson, G. Designing frequency-dependent relaxation rates and Lamb shifts for a giant artificial atom. *Phys. Rev. A* **90**, 013837 (2014).

36. Zhao, W. & Wang, Z. Single-photon scattering and bound states in an atom-waveguide system with two or multiple coupling points. *Phys. Rev. A* **101**, 053855 (2020).

37. Guo, L., Kockum, A. F., Marquardt, F. & Johansson, G. Oscillating bound states for a giant atom. *Phys. Rev. Res.* **2**, 043014 (2020).

38. Cheng, W., Wang, Z. & Liu, Y.-X. Boundary effect and dressed states of a giant atom in a topological waveguide. Preprint at https://arxiv.org/abs/2103.04542 (2021).

39. Vega, C., Porras, D. & González-Tudela, A. Qubit-photon bound states in topological waveguides with long-range hoppings. *Phys. Rev. A* **104**, 053522 (2021).

40. Kockum, A. F., Johansson, G. & Nori, F. Decoherence-free interaction between giant atoms in waveguide quantum electrodynamics. *Phys. Rev. Lett.* **120**, 140404 (2018).

41. Kannan, B. et al. Waveguide quantum electrodynamics with superconducting artificial atoms. *Nature* **583**, 775–779 (2020).

42. Carollo, A., Cilluffo, D. & Ciccarello, F. Mechanism of decoherence-free coupling between giant atoms. *Phys. Rev. Res.* **2**, 043184 (2020).

43. Soro, A. & Kockum, A. F. Chiral quantum optics with giant atoms. *Phys. Rev. A* **105**, 023712 (2022).

44. Ask, A., Fang, Y.-L. L. & Kockum, A.F. Synthesizing electromagnetically induced transparency without a control field in waveguide QED using small and giant atoms. Preprint at https://arxiv.org/abs/2011.15077 (2020).

45. Vadiraj, A. M. et al. Engineering the level structure of a giant artificial atom in waveguide quantum electrodynamics. *Phys. Rev. A* **103**, 023710 (2021).

46. Zhu, Y., Wu, R. & Xue, S. Spatial non-locality induced non-markovian EIT in a single giant atom. Preprint at https://arxiv.org/abs/2106.05020 (2021).

47. Zhao, W., Zhang, Y. & Wang, Z. Phase-modulated Autler-Townes splitting in a giant-atom system within waveguide QED. *Front. Phys.* **17**, 42506 (2022).

48. González-Tudela, A., Muñoz, C. S. & Cirac, J. I. Engineering and harnessing giant atoms in high-dimensional baths: a proposal for implementation with cold atoms. *Phys. Rev. Lett.* **122**, 203603 (2019).

49. Cilluffo, D. et al. Collisional picture of quantum optics with giant emitters. *Phys. Rev. Res.* **2**, 043070 (2020).

50. Longhi, S. Photonic simulation of giant atom decay. *Opt. Lett.* **45**, 3017–3020 (2020).

51. Du, L., Cai, M.-R., Wu, J.-H., Wang, Z. & Li, Y. Single-photon nonreciprocal excitation transfer with non-Markovian retarded effects. *Phys. Rev. A* **103**, 053701 (2021).

52. Du, L. & Li, Y. Single-photon frequency conversion via a giant Λ-type atom. *Phys. Rev. A* **104**, 023712 (2021).

53. Yu, H., Wang, Z. & Wu, J.-H. Entanglement preparation and nonreciprocal excitation evolution in giant atoms by controllable dissipation and coupling. *Phys. Rev. A* **104**, 013720 (2021).

54. Cai, Q. & Jia, W. Coherent single-photon scattering spectra for a giant-atom waveguide-QED system beyond the dipole approximation. *Phys. Rev. A* **104**, 033710 (2021).

55. Du, L., Chen, Y.-T. & Li, Y. Nonreciprocal frequency conversion with chiral Λ-type atoms. *Phys. Rev. Res.* **3**, 043226 (2021).

56. Wang, X. & Li, H.-R. Chiral quantum network with giant atoms. *Quantum Sci. Technol.* **7**, 035007 (2022).

57. Andersson, G., Suri, B., Guo, L., Aref, T. & Delsing, P. Non-exponential decay of a giant artificial atom. *Nat. Phys.* **15**, 1123–1127 (2019).

58. Yuan, L., Shi, Y. & Fan, S. Photonic gauge potential in a system with a synthetic frequency dimension. *Opt. Lett.* **41**, 741–744 (2016).

59. Li, G. et al. Dynamic band structure measurement in the synthetic space. *Sci. Adv.* **7**, eabe4335 (2021).

60. Yu, D., Peng, B., Chen, X., Liu, X.-J. & Yuan, L. Topological holographic quench dynamics in a synthetic frequency dimension. *Light Sci. Appl.* **10**, 209 (2021).

61. Yuan, L., Dutt, A. & Fan, S. Synthetic frequency dimensions in dynamically modulated ring resonators. *APL Photonics* **6**, 071102 (2021).

62. Wendin, G. Quantum information processing with superconducting circuits: a review. *Rep. Prog. Phys.* **80**, 106001 (2017).

63. Blais, A., Girvin, S. M. & Oliver, W. D. Quantum information processing and quantum optics with circuit quantum electrodynamics. *Nat. Phys.* **16**, 247–256 (2020).

64. Yuan, L. & Fan, S. Topologically nontrivial Floquet band structure in a system undergoing photonic transitions in the ultrastrong-coupling regime. *Phys. Rev. A* **92**, 053822 (2015).

65. Scully, M. O. & Zubairy, M. S. *Quantum Optics* (Cambridge Univ. Press, 1997).

66. Shen, J.-T. & Fan, S. Coherent single photon transport in a one-dimensional waveguide coupled with superconducting quantum bits. *Phys. Rev. Lett.* **95**, 213001 (2005).

67. Shen, J.-T. & Fan, S. Strongly correlated multiparticle transport in one dimension through a quantum impurity. *Phys. Rev. A* **76**, 062709 (2007).

68. Calajó, G., Ciccarello, F., Chang, D. & Rabl, P. Atom-field dressed states in slow-light waveguide QED. *Phys. Rev. A* **93**, 033833 (2016).

69. Scigliuzzo, M. et al. Extensible quantum simulation architecture based on atom-photon bound states in an array of high-impedance resonators. Preprint at https://arxiv.org/abs/2107.06852 (2021).

70. Yuan, L., Lin, Q., Xiao, M. & Fan, S. Synthetic dimension in photonics. *Optica* **5**, 1396–1405 (2018).

71. Ozawa, T. & Price, H. M. Topological quantum matter in synthetic dimensions. *Nat. Rev. Phys.* **1**, 349–357 (2019).

72. Lustig, E. & Segev, M. Topological photonics in synthetic dimensions. *Adv. Opt. Photon.* **13**, 426–461 (2021).

73. Lee, N. R. A. et al. Propagation of microwave photons along a synthetic dimension. *Phys. Rev. A* **101**, 053807 (2020).

74. Chen, L.-H., Chen, G., Liu, R. & Wang, X.-H. Dynamically tunable multifunctional QED platform. *Sci. China Phys. Mech. Astron* **62**, 974211 (2019).

75. Peng, B. et al. Parity-time-symmetric whispering-gallery microcavities. *Nat. Phys.* **10**, 394–398 (2014).

76. Jiang, X.-F., Zou, C.-L., Wang, L., Gong, Q. & Xiao, Y.-F. Whispering-gallery micro-cavities with unidirectional laser emission. *Laser Photon. Rev.* **10**, 40–61 (2016).

77. Wallraff, A. et al. Strong coupling of a single photon to a superconducting qubit using circuit quantum electrodynamics. *Nature* **431**, 162–167 (2004).

78. Yin, Y. et al. Catch and release of microwave photon states. *Phys. Rev. Lett.* **110**, 107001 (2013).

79. Pechal, M. et al. Microwave-controlled generation of shaped single photons in circuit quantum electrodynamics. *Phys. Rev. X* **4**, 041010 (2014).

80. Kuzmin, R., Mehta, N., Grabon, N., Mencia, R. & Manucharyan, V. E. Superstrong coupling in circuit quantum electrodynamics. *NPJ Quantum Inf.* **5**, 20 (2019).

81. Phillips, D. F., Fleischhauer, A., Mair, A., Walsworth, R. L. & Lukin, M. D. Storage of Light in Atomic Vapor. *Phys. Rev. Lett.* **86**, 783 (2001).

82. Karpa, L. & Weitz, M. A Stern-Gerlach experiment for slow light. *Nat. Phys.* **2**, 332–335 (2006).

83. Du, L., Zhang, Y., Wu, J.-H., Kockum, A. F. & Li, Y. Giant atoms in a synthetic frequency dimension. *Phys. Rev. Lett.* **128**, 223602 (2022).

ACKNOWLEDGEMENTS

AUTHOR CONTRIBUTIONS

H.X. and L.W. contributed equally to this work. Z.L. and L.Y. conceived the idea and developed an analytical model. H.X., L.W., and Z.L. performed the numerical calculations. X.C. and L.Y. supervised the project. All authors contributed to discussion of the results and writing the paper.

COMPETING INTERESTS

The authors declare no competing interests.

ADDITIONAL INFORMATION

Supplementary information The online version contains supplementary material available at https://doi.org/10.1038/s41534-022-00591-7.

Correspondence and requests for materials should be addressed to Zheng-Hong Li or Luqi Yuan.

Reprints and permission information is available at http://www.nature.com/reprints

Publisher's note Springer Nature remains neutral with regard to jurisdictional claims in published maps and institutional affiliations.